

Finite element in Fluid Assignment-2

Md Tariqul Islam

Date: 05/06/2017

A)

The solution of the Stokes problem has been computed using a uniform structured mesh of Q_2Q_0 , Q_2Q_1 , P_1P_1 and MINI ($P_1^+P_1$) elements, with 20 elements per side, and the results are as follows:

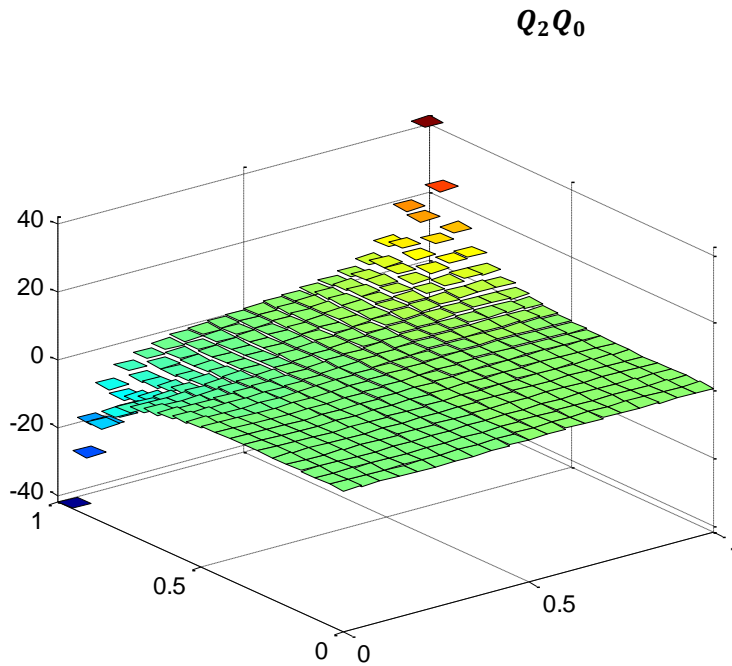


Fig 1: Pressure Field for Q_2Q_0 elements.

The figure above shows reasonable results for the pressure distribution which is expected due to the fact that Q_2Q_0 elements are LBB compliant. At the corners the graph attains a weird behaviour because the elements used for pressure are Q_0 type, which means its discontinuous from element to element.

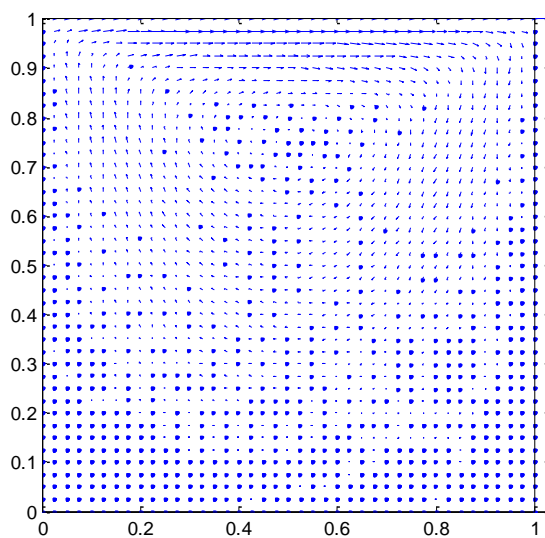


Fig 2: Velocity vectors for Q_2Q_0 elements.

It can be seen from Fig 2 that the velocity is more near the top moving wall compare to rest of the cavity, as the size of the arrows are larger.

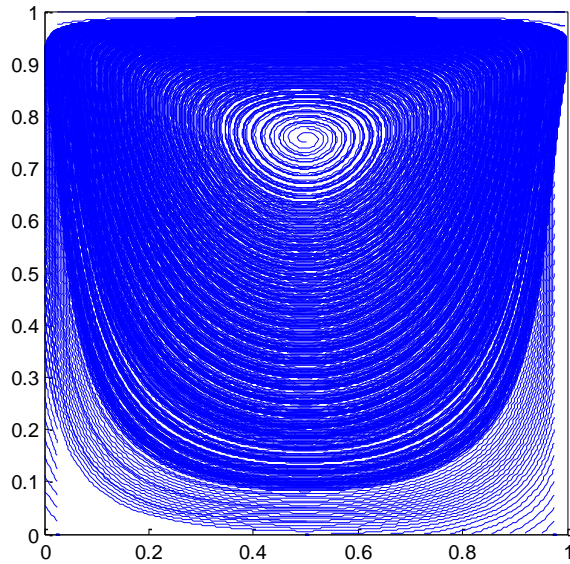


Fig 3: streamlines for Q_2Q_0 elements.

As expected, symmetric streamline is observed in the Fig 3.

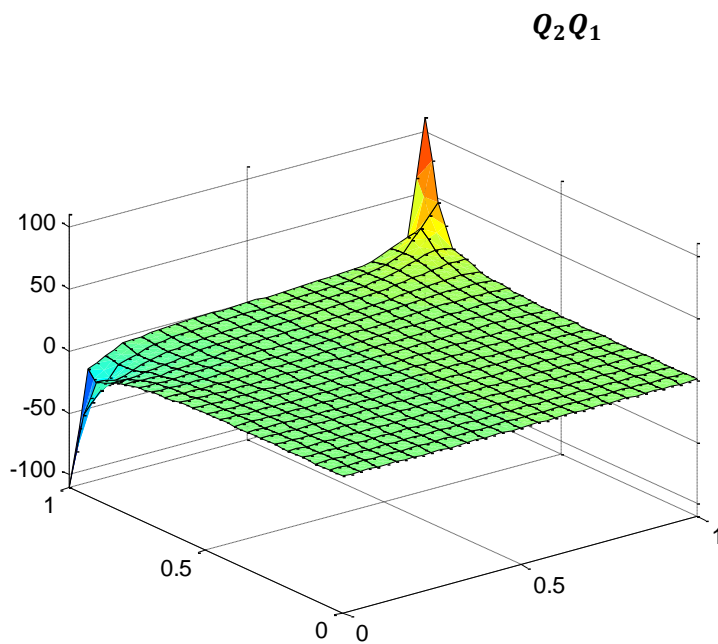


Fig 4: Pressure Field for Q_2Q_1 elements.

The pressure distribution depicted in Fig 4 is well reasonable as the Q_2Q_1 elements are too LBB compliant. There are no weird behaviours at the corners like in Fig 1 as the graphs are much smoother. This is because Q_1 element is used which is linearly continuous.

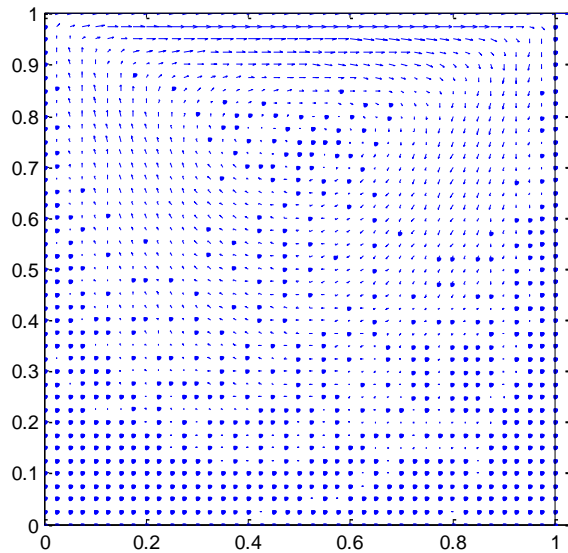


Fig 5: Velocity vectors for Q_2Q_1 elements.

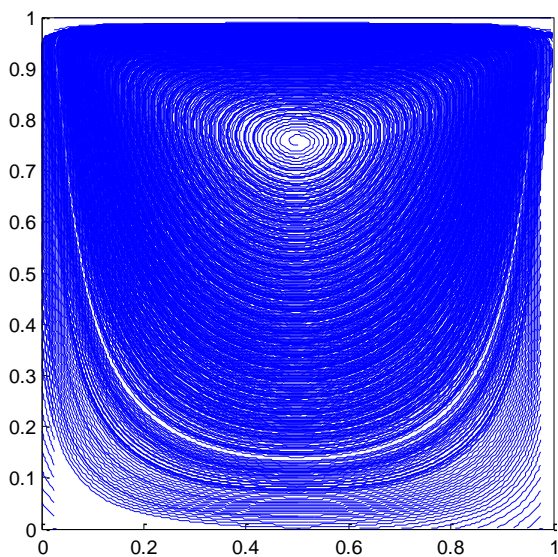


Fig 6: streamlines for Q_2Q_1 elements.

The streamlines are symmetric and velocity vectors are larger near the top walls which is similar to the case of Q_2Q_0 elements.

P_1P_1

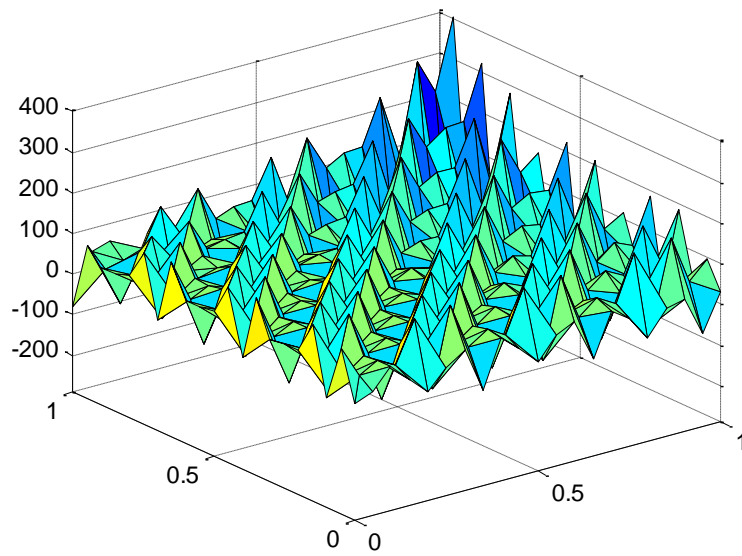


Fig 7: Pressure Field for P_1P_1 elements.

Fig 7 shows the pressure field for the non LBB compliant element P_1P_1 . As expected, they present inaccurate pressure results. They show element to element oscillations and at the corners it is most prominent.

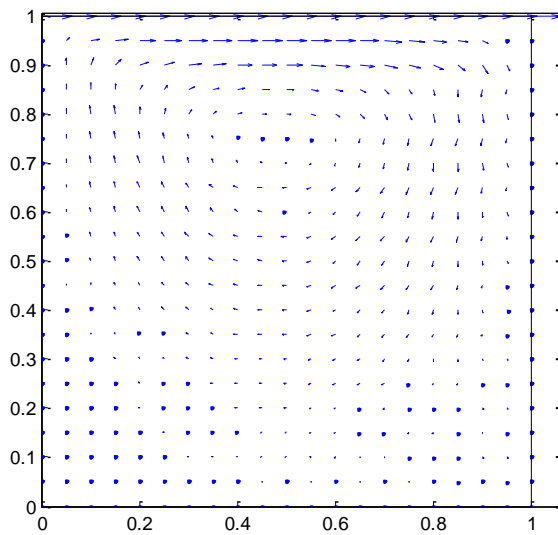


Fig 8: Velocity vectors for P_1P_1 elements.

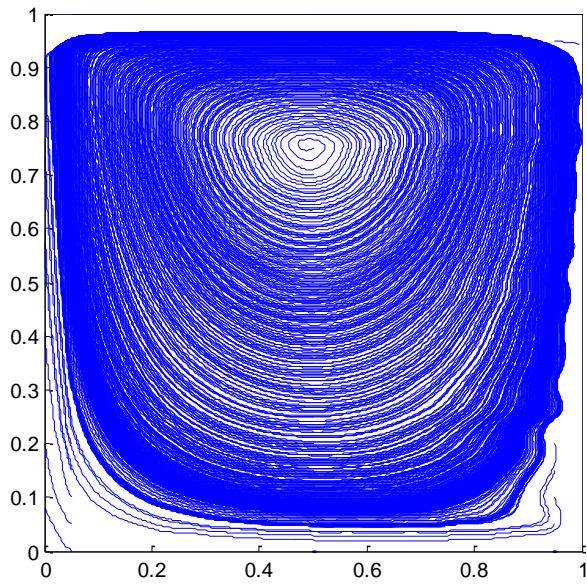


Fig 9: streamlines for P_1P_1 elements.

MINI ($P_1^+P_1$)

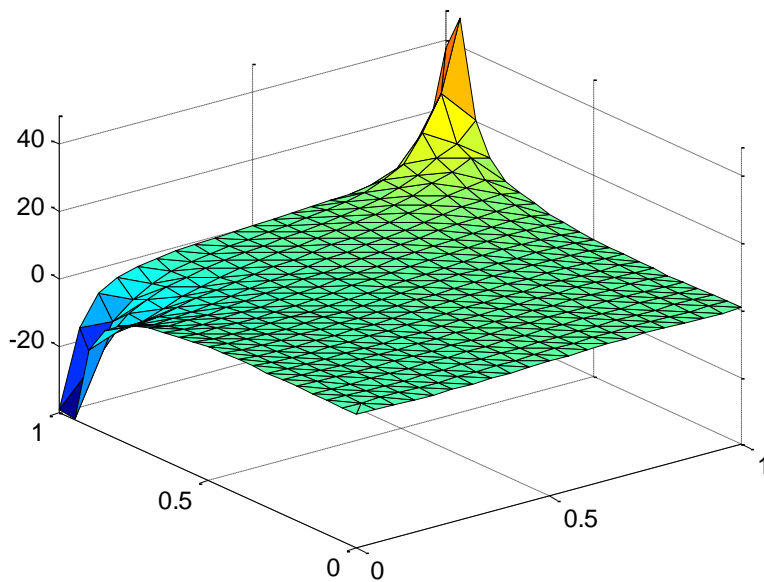


Fig 10: Pressure Field for $P_1^+P_1$ elements.

The MINI element shows similar expected results as Q_2Q_1 element as both are LBB compliant element. There are no oscillations and the result is reasonable.

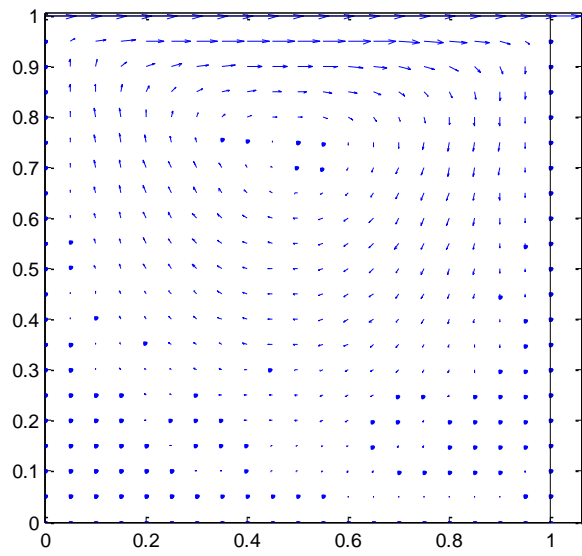


Fig 11: Velocity vectors for $P_1^+P_1$ elements.

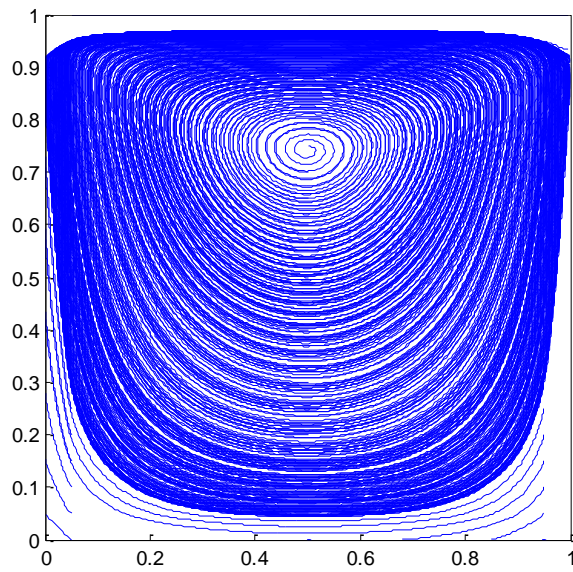


Fig 12: streamlines for $P_1^+P_1$ elements.

B)

Solution of the Stokes problem has been computed considering i) a structured uniform mesh of Q_2Q_1 with element per side ii) a structured mesh of 20×20 Q_2Q_1 element refined near the walls. The results are follows:

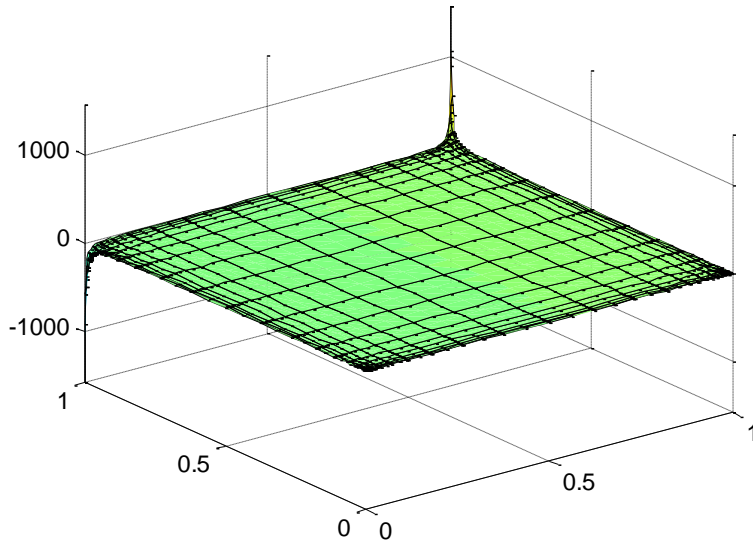


Fig 13: Pressure Field for Q_2Q_1 elements refined near walls

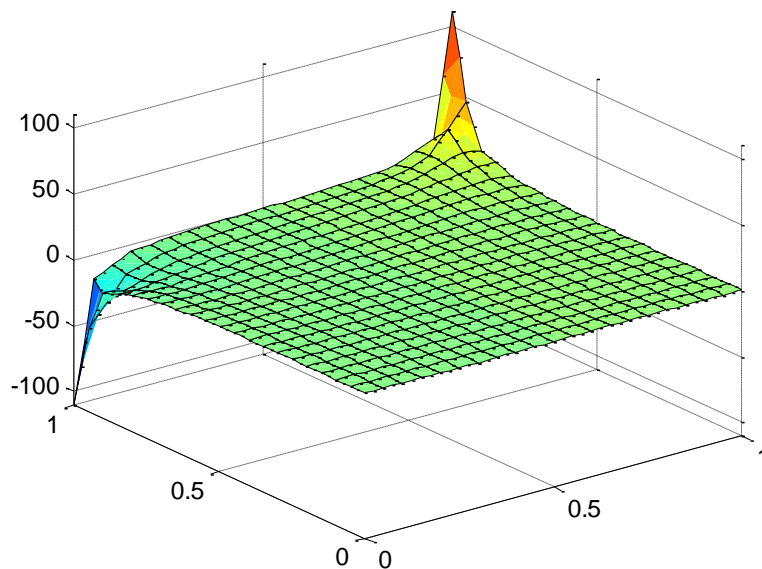


Fig 14: Pressure Field for Q_2Q_1 elements

Figure 13 and 14 shows pressure field for Q_2Q_1 elements with and without refinement near the walls. There is clear difference between the results of these two graphs that used two different meshes. The variation of pressure at the corners is very much minimized when refined meshes are used compare to the coarse mesh where the variation is large. Of course the result for the refined

mesh is more acceptable compare to the other one. This is because, the pressure should have a large value at the corner point only and not in any other point. The plot with the finer mesh behaves more realistically than the other one as it can be seen that the pressure starts to vary only when it goes very near to the corner.

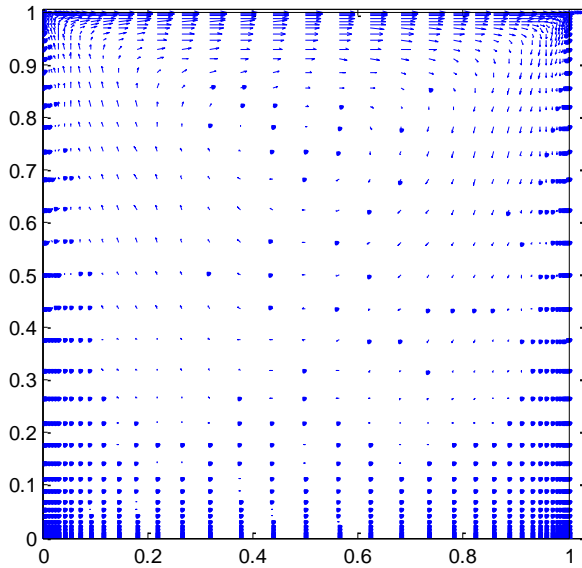


Fig 15: Velocity vectors for Q_2Q_1 elements refined near walls

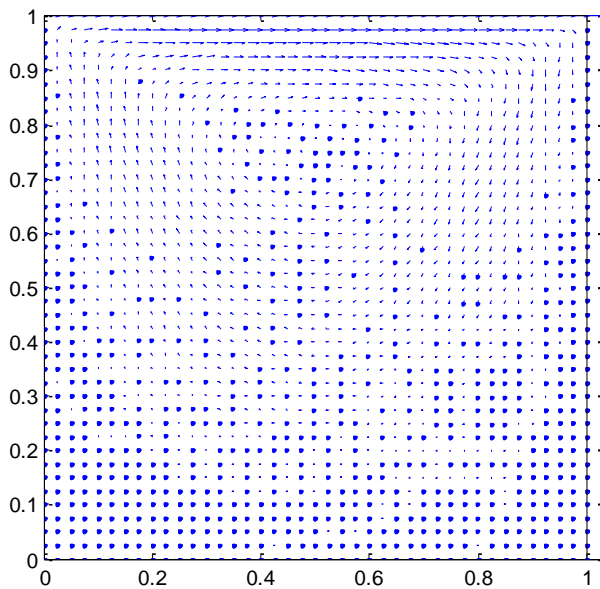


Fig 16: Velocity vectors for Q_2Q_1 elements.

From the figures, it can be seen that the velocity near the top wall becomes more visible once the mesh is refined compare to the unrefined case.

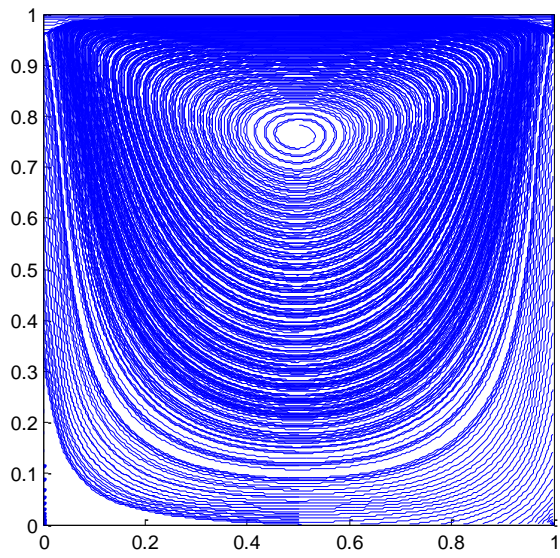


Fig 17: streamlines for Q_2Q_1 elements refined near walls.

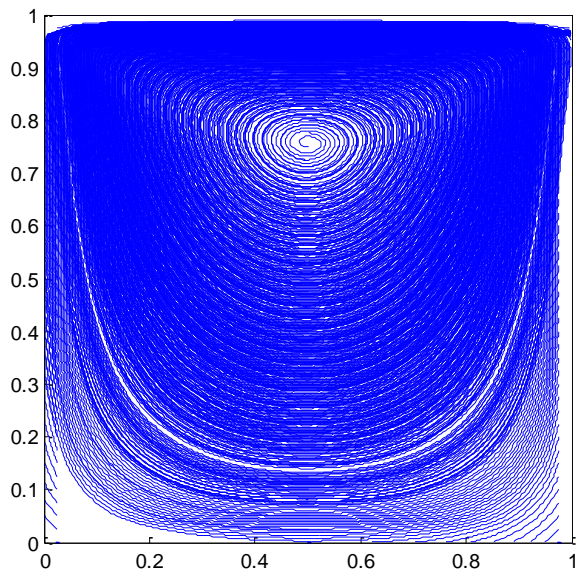


Fig 18: streamlines for Q_2Q_1 elements

C)

The stokes code is modified using GLS stabilized formulation with P_1P_1 elements. The formulation used is the following:

$$a(\mathbf{w}^h, \mathbf{v}^h) + b(\mathbf{w}^h, p^h) = (\mathbf{w}^h, \mathbf{b}^h) + (\mathbf{w}^h, \mathbf{t}^h)_{\Gamma_N},$$

$$b(\mathbf{v}^h, q^h) - \sum_{e=1}^{n_{e1}} \tau_e (\nabla q^h, \nabla p^h)_{\Omega^e} = - \sum_{e=1}^{n_{e1}} \tau_e (\nabla q^h, \mathbf{b}^h)_{\Omega^e}$$

In the weak form of the stokes equation, the stabilized term is incorporated. As linear element is used, the GLS stabilization does not affect the weak form of the momentum equation because the terms involving the second derivatives of the weighting function vanishes. The stabilization parameter used is :

$$\tau_e = \alpha_0 \frac{h_e^2}{4\nu},$$

$$\alpha_0 = 1/3$$

$$\nu = 1$$

The result of the stabilization is as follows:

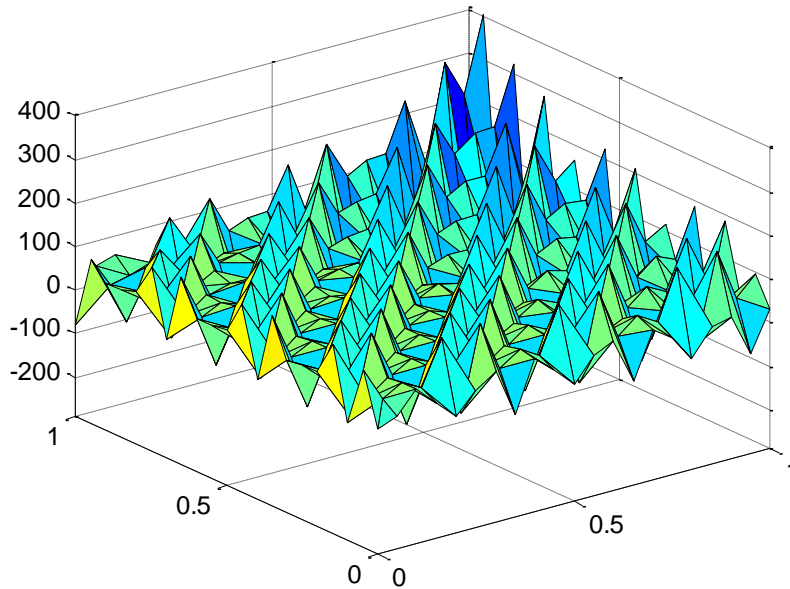


Fig 19: Pressure Field for P_1P_1 elements without stabilization.

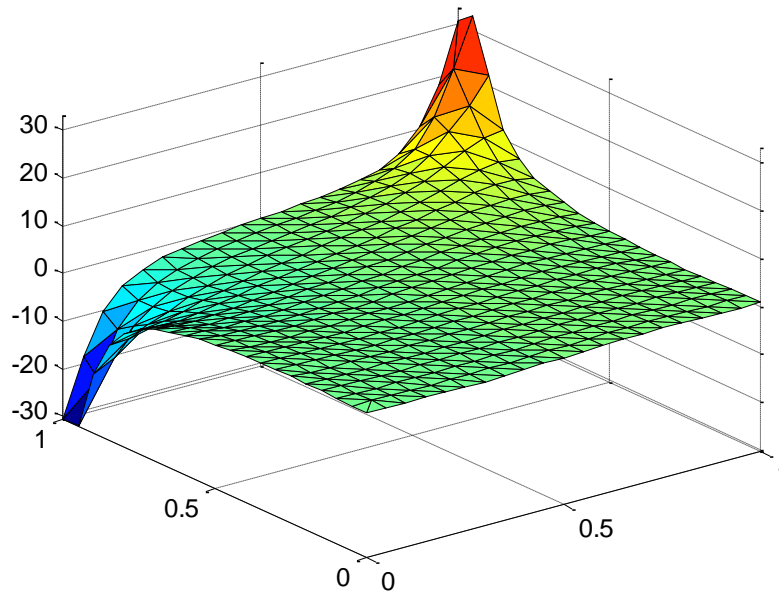


Fig 20: Pressure Field for P_1P_1 elements with stabilization.

As can be seen, the solution is much more practical without any oscillation. The solution became stable. It was expected to behave like this as stabilization term is incorporated to vanish the oscillations.

D)

The Navier-stokes equation is solved using a structured mesh of Q_2Q_1 elements with 20 elements per side considering the Reynold's number being $Re= 100, 500, 1000$ and 2000 .

For each of these Reynold's number, the number of iteration required for the solution to converge are :

| Reynolds number | Number of Iteration |
|-----------------|---------------------|
| 100 | 13 |
| 500 | 29 |
| 1000 | 35 |
| 2000 | 69 |

The results are as follows:

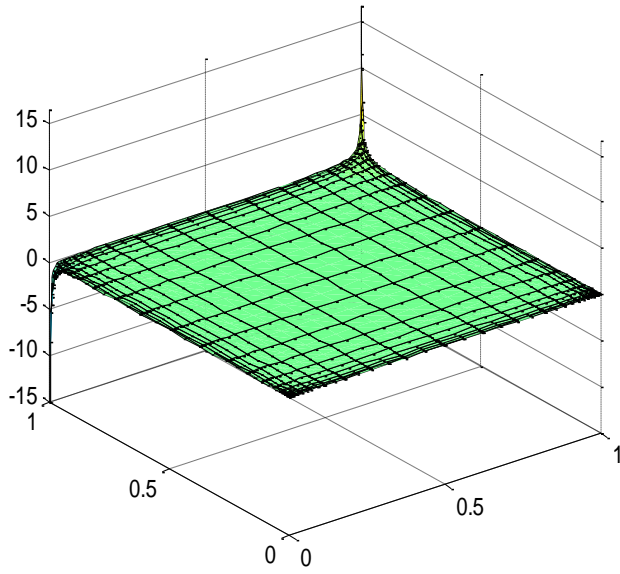


Fig 21: Pressure Field for $Re=100$

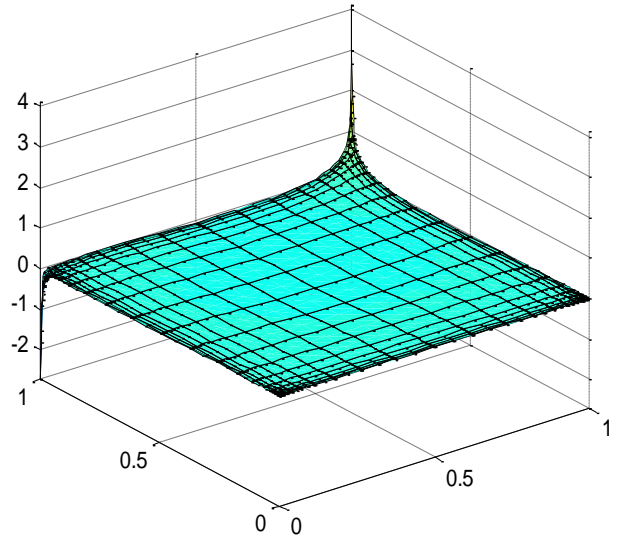


Fig 22: Pressure Field for $Re = 500$

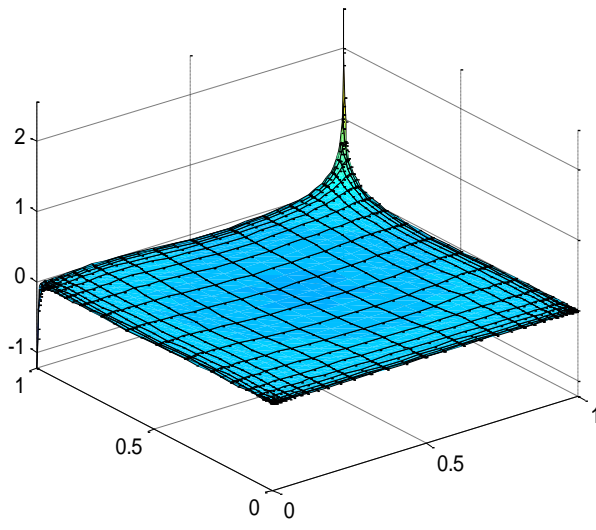


Fig 23: Pressure Field for $Re = 1000$

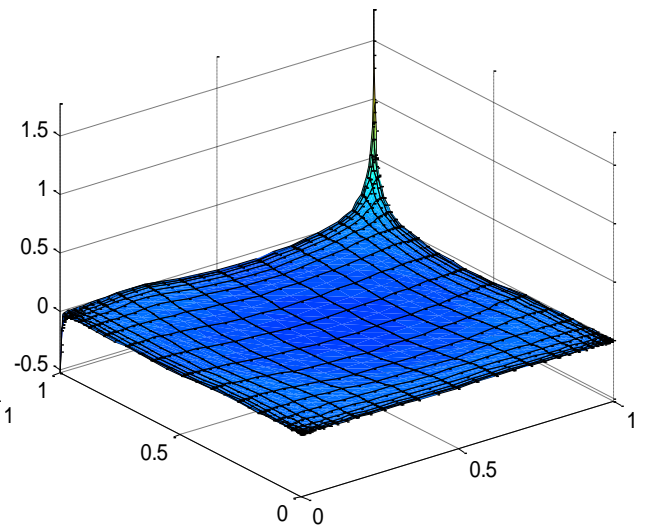


Fig 24: Pressure Field for $Re = 2000$

It can be seen that the variation of the pressure at the corners becomes more prominent as the Reynold's number increases.

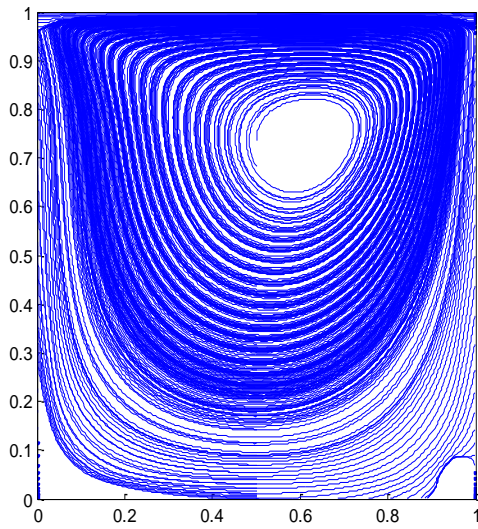


Fig 25: streamlines for $Re = 100$

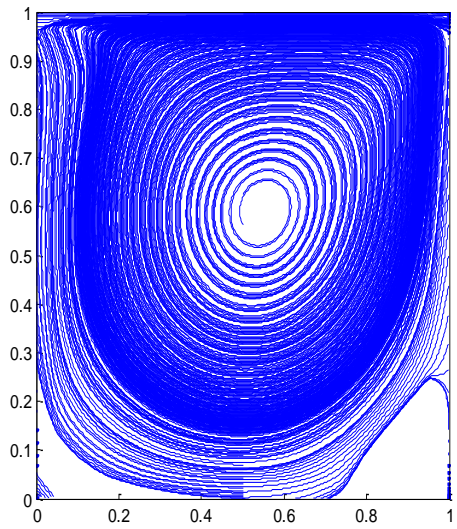


Fig 26: streamlines for $Re = 500$

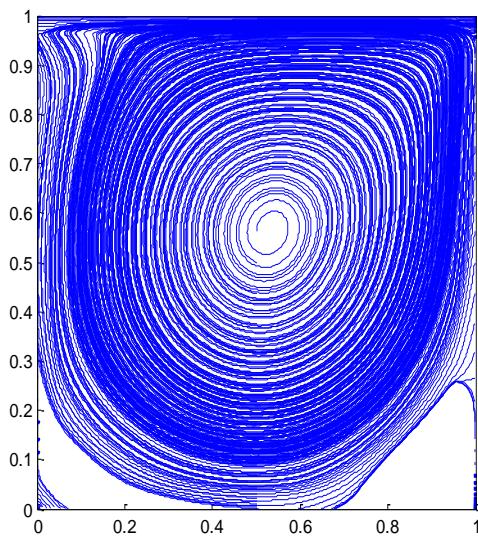


Fig 27: streamlines for $Re = 1000$

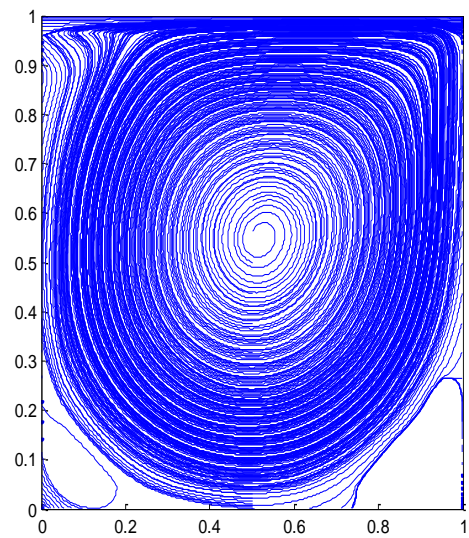


Fig 28: streamlines for $Re = 2000$

As can be seen from the figures, the position of the main vortex moves towards the centre of the cavity when the Reynolds number increases. Also the development of a secondary vortex in the right bottom corner of the cavity becomes apparent and a third vortex appears at the lower left corner. The phenomena completely agrees with the one described in the literature.

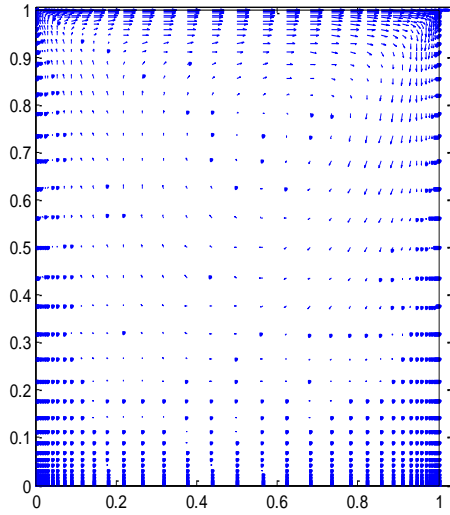


Fig 29: velocity field for $Re = 100$

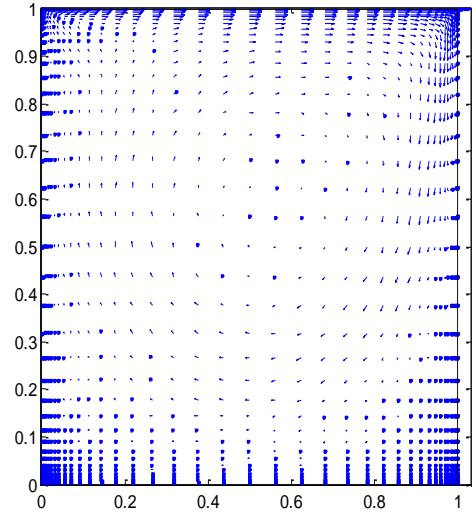


Fig 30: velocity field for $Re = 500$

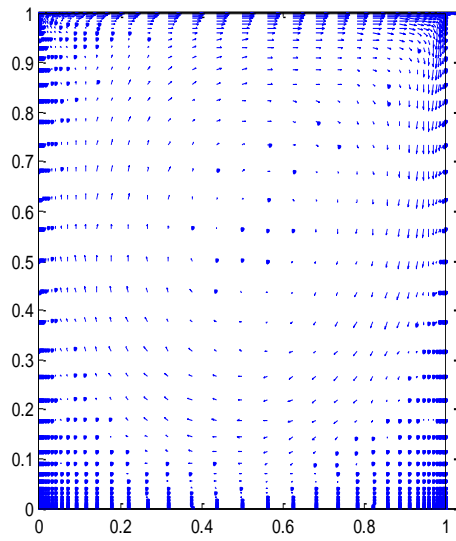


Fig 31: velocity field for $Re = 1000$

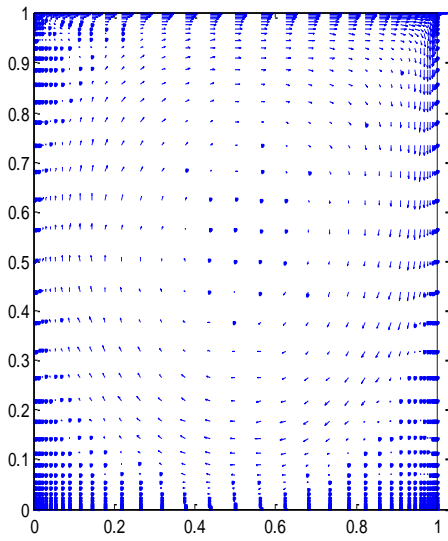


Fig 32: velocity field for $Re = 2000$